

Supplementary models and methods to: Implication of lipid turnover for the control of energy balance

S Bernard¹, K.L. Spalding²

¹Institut Camille Jordan, CNRS, University of Lyon and Inria, 69603 Villeurbanne, France. bernard@math.univ-lyon1.fr

²Department of Cell and Molecular Biology, Karolinska Institutet, 17177 Stockholm, Sweden. kirsty.spalding@ki.se

1 Extended models and methods

Considering that regardless of physiological regulation, energy intake, expenditure and storage are conserved, the total energy intake (EI , in kJ/day) must balance the total energy expenditure (EE , in kJ/day) and energy storage (ES , in kJ/day),

$$EI = EE + ES.$$

The energy storage ES represents the energy imbalance; it can be positive (energy intake greater than expenditure) or negative (energy intake less than expenditure). Excess energy from the diet is stored biochemically in fat and lean tissues, which have their specific energy densities ρ_F and ρ_L .

1.1 Energy in, energy out model (EBM-IOM)

The energy in, energy out model (EBM-IOM, [1]) is a quantitative model for the changes in body weight following changes in energy intake (Figure S2a). Here we briefly present the EBM-IOM as implemented by Hall and colleagues in the body weight planner (<https://www.niddk.nih.gov/bwp>). Modelling details are found in reference [1].

The EBM-IOM partitions the energy imbalance between lean and fat tissue according to an anatomical energy partitioning parameter p . The parameter p depends on the total fat mass. The changes in fat mass (F , in kg) and lean mass (L , in kg) are described by the two ordinary differential equations that track energy imbalance and glycogen (G) fluxes,

$$\frac{dF}{dt} = \frac{1-p}{\rho_F} \left(EI - EE - \rho_G \frac{dG}{dt} \right), \quad (\text{S1})$$

$$\frac{dL}{dt} = \frac{p}{\rho_L} \left(EI - EE - \rho_G \frac{dG}{dt} \right). \quad (\text{S2})$$

The solution for the fat mass is a function of time, taking the value $F(t)$ at time t . Similarly, the lean mass at time t is given by $L(t)$. To obtain unique solutions, initial values must be specified: $F(0) = F_0$ and $L(0) = L_0$. The total body weight (BW , in kg) is the sum of fat and lean mass and glycogen stores.

$$BW = F + L + G. \quad (\text{S3})$$

The initial fat mass is set using a relationship from Jackson et al. [2] that takes into account the body mass index ($BMI = BW/H^2$ kg/m²), total body weight, age and sex.

$$F_0 = \begin{cases} \frac{BW}{100.0}(0.14Age + 37.31 \log(BMI) - 103.94) & \text{in men} \\ \frac{BW}{100.0}(0.14Age + 39.36 \log(BMI) - 102.01) & \text{in women.} \end{cases} \quad (S4)$$

The initial lean mass is obtained from the total body weight, the initial fat mass and the glycogen stores as

$$L_0 = BW_0 - F_0 - G_0. \quad (S5)$$

The anatomical energy partitioning parameter involves a parameter C (in kg) that depends on the Forbes parameter, 10.4kg [3],

$$p(F) = \frac{C}{C + F}, \quad (S6)$$

$$C = 10.4 \frac{\rho_L}{\rho_F}. \quad (S7)$$

The total energy expenditure takes into account the resting metabolic rate (RMR), physical activity (δ), fat (η_F) and lean (η_L) tissue metabolic rates, fat (γ_F) and lean (γ_L) mass coefficients related to the resting metabolic rate, the thermic effect of food (TEF), adaptive thermogenesis (AT), and glycogen metabolism. An aggregated parameter K takes into account non-specific energy expenditure. The total energy expenditure EE is the sum of all the specific expenditures

$$EE = K + \gamma_F F + \gamma_L L + \delta BW + TEF + AT + \eta_F \frac{dF}{dt} + \eta_L \frac{dL}{dt}. \quad (S8)$$

The energy intake is a set parameter that is allowed to depend on time. In the context of the EBM-IOM, it is independent from energy expenditure or other physiological parameters. Given a constant energy intake and an initial energy expenditure, the EBM-IOM predicts that total body weight and composition will adapt, with enough time, to reach energy balance ($ES = 0$).

The thermic effect of food TEF (in kJ/day) is the energy consumed to digest and absorb food. It is proportional to energy intake, with a proportionality constant β_{TEF} ,

$$TEF = \beta_{TEF} EI. \quad (S9)$$

The resting metabolic rate RMR (in kJ/day) is computed by the linear relationship

$$RMR = (9.99BW + 625.0H - 4.92Age + C_{RMR}) \times 4.184, \quad (S10)$$

$$C_{RMR} = \begin{cases} 5.0 & \text{in men,} \\ -161.0 & \text{in women.} \end{cases} \quad (S11)$$

The physical activity level (PAL , unitless) is defined as the ratio between the energy intake and the resting metabolic rate, at energy balance,

$$EI(0) = RMR(0)PAL. \quad (S12)$$

The physical activity expenditure δ (kJ/kg body weight/day) is the energy expenditure per kg body weight outside the thermic effect of food and resting metabolism

$$\delta = ((1 - \beta_{TEF})PAL - 1) \frac{RMR}{BW}. \quad (S13)$$

The parameter K (kJ/day) is determined by assuming initial energy balance $EI(0) = EE(0)$. This implies that

$$K = RMR - \gamma_F F - \gamma_L L. \quad (\text{S14})$$

In addition to the fat and lean mass, energy is stored in muscles and liver as glycogen. The glycogen stores (G , in kg) depend on total carbohydrate intake and use. Carbohydrate intake is calculated as the product between the total energy intake and the percentage of energy coming from carbohydrates c . Glycogen stores are depleted at a rate proportional to G^2 , with a proportionality constant k_G . Glycogen has an energy density ρ_G , and changes in glycogen stores are given by the equation

$$\frac{dG}{dt} = \frac{1}{\rho_G} EI \frac{c}{100} - k_G G^2, \quad (\text{S15})$$

with initial value $G_0 = G_0$. The proportionality constant k_G (in kJ/day kg²) is set by an initial equilibrium assumption $dG/dt = 0$:

$$k_G = EI(0) \frac{c(0)}{100} G_0^2. \quad (\text{S16})$$

Adaptive thermogenesis (AT , in kJ/day) is a transient physiological response to energy imbalance. It acts on a timescale τ_{AT} (in days). Adaptive thermogenesis produces heat from extra energy intake (or reduces heat in case of negative energy balance) with a proportionality constant β_{AT} . Changes in adaptive thermogenesis are given by the equation

$$\frac{dAT}{dt} = \frac{1}{\tau_{AT}} (\beta_{AT} (EI - EE) - AT), \quad (\text{S17})$$

with an initial value $AT(0) = 0$ (equilibrium assumption).

1.2 Carbohydrate-insulin model (CIM)

The carbohydrate-insulin model (CIM) posits that energy partitioning between expenditure and storage is influenced by dietary macro-nutrient composition. In a recent article, Ludwig and colleagues [4] state that the diet influences substrate partitioning. Rapidly digested carbohydrates act through insulin and other hormones to increase fat deposition and limit fat oxidation, driving positive energy balance. Since total energy must be conserved, this means that in the CIM, a lower energy availability must translate into a higher energy intake, or a lower energy expenditure. Ludwig and colleagues observe that when fuel availability decreases, hormonal effects on metabolic pathways, or compensatory mechanisms, such as the resting energy expenditure, muscular efficiency, or physical activity levels, may affect total energy expenditure. Implicitly, this could mean that a higher energy availability would translate into higher energy expenditure.

We propose that the CIM can be articulated within the EBM-IOM framework. Metabolic fuels from food are partitioned amongst different tissues and between the metabolic pathways that lead to storage or oxidation (Supplementary Figure S1). Without assuming any causal or temporal control, if we distinguish between lean and fat tissues, energy is allocated according to three partition parameters. There is not a unique set of parameter that can describe energy allocation, but one choice is: one parameter for allocating fuel for metabolic pathways (oxidation or storage, PSP), one for allocating storage to different anatomical locations (AEP, the anatomical energy partitioning parameter p), and one for allocating metabolic fuel to different tissues (TMP).

We assume that the dietary glycaemic load (GL) is the main driver of the differences between the CIM and the EBM-IOM. According to the CIM, a high-GL shifts the energy partition towards

fat storage. The “shift in energy partition towards fat storage” can be interpreted in the following ways: i) A high GL shifts the anatomical energy partitioning parameter p towards fat storage, i.e. the fraction p of energy stored in the lean mass is decreasing (Supplementary Figure S1, AEP). In this interpretation, the amount of energy storage is not directly affected. We refer to this interpretation as the anatomical partitioning of energy storage mechanism (CIM-APES). (Figure S2b). ii) A high GL favour energy storage, causing energy imbalance that can be compensated by an increased energy intake and/or a decreased energy expenditure. In this interpretation, under a high carbohydrate intake, the primary substrate partitioning is shifted to favour energy storage (Supplementary Figure S1, PSP). The anatomical energy partitioning parameter p is not affected. We refer to this interpretation as the energy deposition mechanism (CIM-EDM) (Supplementary Figure S2c).

For the CIM-APES to be coherent with the CIM, we need to make the following assumptions

- During positive energy imbalance (weight gain), the anatomical energy partitioning parameter must be a decreasing function of the GL. This ensures that during weight gain on a high GL diet, energy storage goes preferentially to fat mass.
- During negative energy imbalance (weight loss), the anatomical energy partitioning parameter must be an increasing function of the GL. This ensures that during weight loss on a low GL diet, fat mass is preferentially lost.

Combined together, these two assumptions have several interesting implications. Firstly, at energy balance, the anatomical energy partitioning parameter should remain constant. This is not in agreement with the CIM, because the CIM predicts that dietary carbohydrate intake has an effect on energy balance even in isocaloric diets. Secondly, the anatomical energy partitioning parameter must depend not only on the GL, but also on the difference between the energy intake and the energy expenditure. It is not clear how this could be controlled physiologically. One could argue that energy balance is never satisfied; energy is in excess in postprandial periods, and is in deficit during fasting. A fine regulation of energy storage and mobilisation under the CIM-APES would act as a ratchet: Following a high GL meal, excess energy would be stored as fat. During the late-postprandial and fasting period, energy would be mobilized from the lean mass, meaning in the long run a high GL diet would lead to a decrease in lean mass, and an increase in fat mass. Conversely, in the long run, a low GL diet would lead to an increase in lean mass, and a decrease in fat mass.

For the CIM-EDM to be coherent with the CIM, we need to make the following assumption

- The total (net) energy storage increases with the GL, independently of any other factors.

This interpretation has also several interesting implications. Firstly, the energy expenditure is limited by the available energy not being stored. This means that energy expenditure should decrease in high GL diets. Secondly, energy expenditure should increase in low GL diets, as energy storage decreases. Consequently, energy balance follows from energy storage, in line with the reversal of causality proposed in the CIM. The deposit model does not specify whether the anatomical energy partitioning parameter is affected by dietary carbohydrates. The CIM-APES and the CIM-EDM are not mutually exclusive, and we have considered a combined APES/EDM, called CIM-PDM. However, the CIM-APES alone does not provide the necessary mechanisms to reproduce correctly one the main predictions of the CIM, namely that compared to a high carbohydrate intake diet, a low carbohydrate diet increases energy expenditure independently of total energy intake [4].

Anatomical partitioning of energy storage mechanism (CIM-APES)

We implemented the CIM-APES as follows. We assume that the parameter C in equation (S6) is modulated by the GL and the sign of the energy imbalance. Determining the sign of the energy imbalance is not trivial, because the energy expenditure depends itself on the anatomical energy partitioning parameter p , through the tissue specific metabolic rates. Therefore, we use the adaptive thermogenesis (AT , equation (S17)) as a proxy the sign of energy imbalance. The parameter C becomes $C\beta_{GL}$, where the function β_{GL} is

$$\beta_{GL}(GL, AT) = \begin{cases} a_{FP} + (2 - 2a_{FP})\frac{GL_{STD}^2}{GL_{STD}^2 + GL^2} & AT > 0, \\ a_{FP} + (2 - 2a_{FP})\frac{GL^2}{GL_{STD}^2 + GL^2} & AT \leq 0, \end{cases} \quad (S18)$$

The parameter θ is the GL value at which the effect is neutral with respect to the EBM-IOM: $\beta_{GL}(\theta, AT) = 1.0$ The parameter a is the minimal value of β_{GL} can take, and $2 - a$ is the maximal value of β_{GL} We used a value of $a = 0.5$. Therefore, the value of the parameter C is modulated between $0.5C$ and $1.5C$. The anatomical energy partitioning parameter becomes

$$p(F) = \frac{C\beta_{GL}(GL, AT)}{C\beta_{GL}(GL, AT) + F}. \quad (S19)$$

Energy deposition mechanism (CIM-EDM)

We implemented the CIM-EDM as follows. To take into account the decrease in energy availability, we introduce an energy shift factor $\beta_{ED} > 0$ (unitless) that depends on dietary GL. In the EBM-IOM, the GL has a constant effect, so there must be a GL value for which the amount of energy available is equal to the EBM-IOM-based energy expenditure. Let EE_{50} be this value of energy expenditure. The value of EE_{50} depends on the GL through the thermic effect of food, so it must be computed by a non-linear fixed point equation. Similarly, there is a fixed-point energy intake EI_{50} that corresponds to energy intake in the EBM-IOM and the CIM. We make the additional assumption that the fixed-point EE_{50} and EI_{50} correspond roughly to a 50% carbohydrate intake and a GL equal to GL_{STD} . That is, we make the assumption that the EBM-IOM was calibrated for a 50% carbohydrate intake. The real figure might be slightly different, but for the purpose of the model, it is the difference in carbohydrate intake from the fixed-point level that matters, not the absolute value. The factor β_{ED} shifts the energy allocation between expenditure and storage, so that the effective energy expenditure becomes

$$EE = \beta_{ED}EE_{50}. \quad (S20)$$

A shift factor between 0 and 1 results in an CIM EE lower than the fixed-point energy expenditure EE_{50} . A shift factor greater than 1 results in an EE higher than the fixed-point energy expenditure.

We call the energy deposit, denoted ED (in kJ/day), the difference between EE_{50} and the EE,

$$ED = (1 - \beta_{ED})EE_{50}. \quad (S21)$$

A positive value is the amount of energy that would be needed to cover daily physiological needs, but is not available as fuel. A negative value is interpreted as an energy surplus that will not be stored. We assume that the energy deposit is covered up to a fixed factor g_{ED} (unitless) by an increase in energy intake. The total daily energy intake under CIM, EI (in kJ/day), becomes

$$EI = EI_{50} + g_{ED}ED, \quad (S22)$$

In case of an energy surplus, the energy intake is reduced. In the CIM, the total energy storage (neglecting change in glycogen stores) is $ES = EI - EE$. When re-expressed in terms of the fixed-point energy expenditure EE_{50} and energy intake EI_{50} , the energy storage for the CIM becomes $ES = EI_{50} - EE_{50} + (1 + g_{ED})ED = ES_{50} + (1 + g_{ED})ED$. Therefore, when the EBM-IOM predicts energy balance ($EI_{50} = 0$), the CIM energy storage becomes proportional to the energy deposit ED.

The shift factor, $\beta_{ED}(GL)$ (unitless), is a function of the dietary GL that depends on several hormonal and physiological mechanisms that have at most been partially quantified. Quantifying these mechanisms is out of the scope of this study. Nevertheless, based on the CIM, β_{ED} should be a decreasing, but positive function of the GL, that is, a higher GL should lead to a lower EE. GL is based on the glycaemic index (GI) that provides an equivalence between different carbohydrates and glucose. Reported daily GL values range between 50 and 200 g equivalent-sugar per day [5, 6]. For a medium $GL = GL_{STD}$, the energy intake in the CIM and the EBM-IOM should be the same, and β_{ED} should be close to one. We also assume that β_{ED} is bounded above and below by β_{ED}^{max} and β_{ED}^{min} . We define the function β_{ED} as

$$\beta_{ED}(GL) = \beta_{ED}^{min} + (\beta_{ED}^{max} - \beta_{ED}^{min}) \frac{GL_{STD}}{GL_{STD} + GL}. \quad (S23)$$

The EBM-IOM can be simulated in the context of the CIM by setting $\beta_{ED}(GL) = 1.0$.

The GL can be computed from the fraction of the total energy intake in carbohydrate, converted to grams sugar equivalent through the glycaemic index. Using an energy density of 17 kJ/g for carbohydrates, the GL is

$$GL = \frac{c}{100} \frac{EI}{17.0} \frac{GI}{100}. \quad (S24)$$

For instance, a diet of 10,000 kJ/day, with an average GI of 45 (corresponding to whole wheat) and 65% of energy from carbohydrate, would have a GL of 172 g sugar-equivalent per day. However, the GL cannot be computed using equation (S24), because the energy intake depends itself on the GL in a nonlinear way through the function β_{ED} . To circumvent this problem, we pose a differential equation on GL , much in the same fashion as for AT (equation (S17)). We assume that GL adapts to energy intake on a timescale τ_{GL} , relative to a standard glycaemic load GL_{STD} ,

$$\frac{dGL_{CIM}}{dt} = \frac{1}{\tau_{GL}} \left(\frac{c}{c(0)} GL_{STD} \frac{EI}{EI(0)} - GL_{CIM} \right), \quad (S25)$$

with an initial value $GL_{CIM}(0) = GL_{STD}$. When the carbohydrate fraction and energy intake are constant, the GL stays constant as well. Here we neglect a possible additional feedback loop on the GL, by which low fuel availability would drive a craving for high-glycaemic index food.

The fixed-point energy expenditure depends in part on energy intake, through TEF (equation (S9)), AT (equation (S17)), and tissue metabolic rates. In the CIM, there are additional functional dependencies between energy intake and expenditure: the energy expenditure depends on the GL, which depends itself on the energy intake, which in turn depends on the energy expenditure (equation (S22)). The additional dependency of the GL on energy intake has been removed through equation (S25). After solving equation (S8) with these dependencies, we obtain a closed form

formula for the fixed-point energy expenditure EE_{50} ,

$$\begin{aligned}
A_1 &= p \frac{\eta_L}{\rho_L} + (1-p) \frac{\eta_F}{\rho_F}, \\
A_2 &= K + \gamma_F F + \gamma_L L + \delta BW + \beta_{TEF} EI_{50} + AT, \\
A_3 &= (1 + A_1 - g_{ED}(1 - \beta_{ED})(\beta_{TEF} + A_1)), \\
EE_{50} &= \frac{A_2 + ((1 - c/100)EI_{50} + k_g G^2)A_1}{A_3(1 + \frac{c/100 g_{ED}(1 - \beta_{ED})A_1}{A_3})}. \tag{S26}
\end{aligned}$$

The EBM-IOM provides a passive negative feedback loop that tends to stabilize body weight, and a feed-forward loop that causes energy storage from high energy intake (Figure S2a). The CIM-EDM reverses the causality on energy storage: energy deposition as fat, mediated by the increase in the ratio of insulin-to-glucagon, causes an imbalance between energy intake and expenditure, but preserves the EBM-IOM feed-forward loop. In some descriptions of the CIM, energy storage fully determines energy imbalance, suggesting that there is no EBM-IOM feed-forward loop at all [7, 8]. We argue here that the EBM-IOM feed-forward loop is not only compatible with the main ideas of CIM, but is also essential to its key features. Together with the feed-forward loop, the CIM-EDM closes a positive feedback loop [9], which amplifies the effects of small changes in dietary macro-nutrients. In the absence of the feed-forward loop, the decrease in energy expenditure and the increase in energy intake due to craving would have no effect on energy storage. A full reversal mechanism, denoted CIM-REV, requires to cut the feed-forward loop (Figure S2d). A description of the CIM-REV is given below.

Partition/deposition mechanism (CIM-PDM)

The CIM-PDM combines the CIM-APES and the CIM-EDM. The factor a_{FP} was restricted to 0.95, as numerical instabilities appeared in some virtual subjects for smaller values.

Reversal in causation (CIM-REV)

The CIM-REV assumes that energy imbalance is fully determined by the GL in that only the GL, and not the energy intake, determines energy storage. To do that we replaced the energy imbalance term $EI - EE$ in equations (S1) and (S2) by the energy deposit ED . This implies that $ES_{50} = 0$, disconnecting the EBM-IOM feed-forward loop. In the CIM-REV, energy balance is independent of the energy intake, and therefore does not conserve energy. We limited the CIM-REV to the short trial, because simulations over longer durations lead to non-physical solutions, such as negative energy.

1.3 Lipid turnover

Most of the fat mass is located in the adipose tissue, with a small fraction in the liver and muscles. Here we assume that the total fat mass F are triglycerides stored in the adipose tissue. Neither the EBM-IOM or the CIM specify how triglyceride storage and release from the adipose tissue is regulated. Energy conservation implies only that unused energy is stored, and that energy is mobilized during negative energy imbalance. Lipid storage (K_{in} , in kg/day) and mobilisation (K_{out} , per day) occur on a daily basis even in weight stable individuals, suggesting that a significant fraction of energy intake is stored, and that daily energy needs are covered in part by lipolysis of fat stores. At fat mass balance, the rate of lipid exchange (per day) is termed lipid turnover. From a lipid turnover viewpoint, a change in the total fat mass F is given by the balance equation

$$\frac{dF}{dt} = K_{in} - K_{out}F. \tag{S27}$$

This equation is strictly equivalent to the EBM-IOM formulation (S1). This means that (neglecting change in glycogen stores)

$$\frac{1-p}{\rho_F}(EI - EE) = K_{in} - K_{out}F.$$

Even though it is tempting to do so, there is no reason to identify EI to K_{in} , and EE to $K_{out}F$. Nevertheless, some constraints must be satisfied. If $ES > 0$, K_{in} must be larger than the net increase in fat storage, then

$$K_{in} > \frac{1-p}{\rho_F}(EI - EE).$$

Conversely, if $ES < 0$, K_{out} must be larger than the net amount of fat mobilized, then

$$K_{out} > \frac{1-p}{\rho_F}(EE - EI),$$

These two inequalities provide minimal bounds on how much fat can be gained and lost. However, in weight loss conditions, these inequalities are of little use. Instead we use the observation that in obese individuals, the lipid storage rate is strongly correlated to BMI , but not so much in individuals without obesity (Suppl. 2 Fig. 2B in reference [10]). This suggests that K_{in} increases with BMI , or more plausibly, with total fat mass. Therefore, we assume that lipid storage to adipose tissue is at least proportional to energy intake, with a non-constant factor $\beta_{uptake}(\phi_0 + \phi_1 F)$,

$$K_{in} = \max\left\{\frac{\beta_{uptake}}{\rho_F}(\phi_0 + \phi_1 F)EI_{CIM}, \frac{dF}{dt}\right\} \quad (S28)$$

where the term dF/dt is evaluated using equation (S1).

We define lipid age A_F as the mean residence time in years of the triglycerides in the adipose tissue. Using the methodology proposed recently (equation (13) in [11]), lipid age dynamics follow the equation

$$\frac{dA_F}{dt} = \frac{1}{365} - \frac{K_{in}}{F}A_F \quad (S29)$$

(where the ratio 365 converts the lipid age from days to years). The initial value is set to the equilibrium state

$$A(0) = \frac{F_0}{365K_{in}(0)}. \quad (S30)$$

The lipid mobilisation rate (K_{out} , per day) follows from the mass balance equation

$$\frac{dF}{dt} = K_{in} - K_{out}F.$$

After solving for K_{out} , we obtain the following relationship

$$K_{out} = \frac{K_{in} - \frac{dF}{dt}}{F}, \quad (S31)$$

where the term dF/dt is evaluated using equation (S1).

Supplementary Table S1. Parameter values and constants.

| Parameter | Value | Unit | Note |
|--------------------|--------|--------------------|---|
| ρ_F | 39.5e3 | kJ/kg | energy density of fat tissue |
| ρ_L | 7.6e3 | kJ/kg | energy density of lean tissue |
| ρ_G | 17.6e3 | kJ/kg | energy density of glycogen |
| γ_F | 13.0 | kJ/kg/day | regression coefficients relating resting metabolic rate vs body fat |
| γ_L | 92.0 | kJ/kg/day | regression coefficients relating resting metabolic rate vs lean mass |
| η_F | 750.0 | kJ/kg | biochemical efficiencies of fat |
| η_L | 960.0 | kJ/kg | biochemical efficiencies of proteins |
| β_{TEF} | 0.1 | unitless | 10% TEF typical assumption |
| β_{AT} | 0.14 | unitless | adaptive thermogenesis coefficient |
| τ_{AT} | 14.0 | day | adaptive thermogenesis timescale |
| c | 50 | percent | US guidelines 45%–65%; simulation range 10%–90% |
| G_0 | 0.5 | kg | initial glycogen store |
| τ_{GL} | 1.0 | day | manually calibrated |
| GL_{STD} | 125 | g equiv. sugar/day | GL corresponding to $c = 50\%$ |
| β_{ED}^{max} | 1.1 | unitless | energy deposition factor, manually calibrated |
| β_{ED}^{min} | 0.9 | unitless | energy deposition factor, manually calibrated |
| g_{ED} | 1.0 | unitless | simulation range 0.0–1.0 |
| a_{FP} | 0.4 | unitless | GL factor for anatomical energy partitioning ($a_{FP} = 0.95$ for CIM-PDM) |
| ϕ_0 | 0.5 | unitless | lipid uptake factor, manually calibrated |
| ϕ_1 | 0.015 | kg ⁻¹ | lipid uptake factor, manually calibrated |

1.4 Numerical simulations

The full system of equations is given by six equations (S1), (S2), (S15), (S17), (S25), and (S29). Model parameters can be grouped into four categories: parameters that can be set by equilibrium assumptions, physiological constants that have values reported in the literature, parameters that are specific to individuals, and parameters for which no information is available. Energy expenditure and storage regulation in the CIM are controlled by β_{ED} . The EBM-IOM is simulated by setting $\beta_{ED} = 1$.

1.5 Generation of virtual cohorts

We generated two cohorts (Cohort V1 and V2) of virtual subjects based on two clinical cohorts published by Arner et al. [11]. Cohort 1 consisted of 54 individuals with a mean follow-up time of 13 years (Table S2). Cohort 2 consisted of 41 individuals with obesity who underwent bariatric surgery, with a 5 year follow-up (Table S3). Most of the clinical subjects were women. For this reason, the virtual cohorts include only women. Individual initial body weight (BW_0), height (H), age (Age_0) and measured K_{in} were used to generate ground statistical characteristic of the virtual cohort. Each individual is characterised by a random parameter set ($BW_0, H, PAL, c_0, \beta_{uptake}$).

A total of $N = 1000$ random parameter sets were generated for each virtual cohort according to distributions in Table S2 (cohort V1) and Table S3 (cohort V2). An initial scan of the cohorts was used to remove virtual subjects with a BMI or height outside the range of clinical cohorts. The cohort size was reduced to $n=938$ for cohort V1, and to $n=687$ for cohort V2.

Two models were simulated: CIM and EBM-IOM. In the CIM, β_{ED} is given by equation (S23). In the EBM-IOM $\beta_{ED} = 1$. We assumed that before year 0, all individuals had a medium carbohydrate intake diet (c_0 normally distributed around 50%, with a standard deviation of 10%). This corresponds to a GL of around 125g sugar equivalent per day, assumed to have a neutral effect in the CIM. We also assumed that all individuals were at energy balance before year 0. This implies $EE = EI$. At the start of the numerical simulations, carbohydrate intake was set to a value ranging

Supplementary Table S2. Nominal parameter distributions of virtual cohort V1. All parameter vectors were drawn from independent samples.

| Parameter | Distribution | Mean | STD | Unit | Note |
|------------------|--------------|------|-------|----------|--|
| BW_0 | Gaussian | 99.2 | 19.2 | kg | cohort 1, initial body weight |
| H | Gaussian | 1.70 | 0.08 | m | cohort 1, height |
| Age_0 | Gaussian | 38.4 | 7.29 | year | cohort 1, initial age |
| PAL | Gaussian | 1.6 | 0.3 | unitless | from cohort 1, physical activity level |
| c_0 | Gaussian | 50.0 | 10.0 | percent | US Guidelines, percent energy from carbohydrates |
| β_{uptake} | Beta | 0.16 | 0.10 | unitless | cohort 1 and equation (S28), energy fraction daily lipid storage |
| ΔEI | Gaussian | 0.0 | 100.0 | kJ/day | change in nominal energy intake |

Supplementary Table S3. Nominal parameter distributions of virtual cohort V2. All parameter vectors were drawn from independent samples.

| Parameter | Distribution | Mean | STD | Unit | Note |
|------------------|--------------|-------|------|----------|--|
| BW_0 | Gaussian | 118.5 | 16.7 | kg | cohort 2, initial body weight |
| H | Gaussian | 1.65 | 0.08 | m | cohort 2, height |
| Age_0 | Gaussian | 42.6 | 9.4 | year | cohort 2, initial age |
| PAL | Gaussian | 1.6 | 0.3 | unitless | from cohort 2, physical activity level |
| c_0 | Gaussian | 50.0 | 10.0 | percent | US Guidelines, percent energy from carbohydrates |
| β_{uptake} | Beta | 0.1 | 0.1 | unitless | cohort 2 and equation (S28), energy fraction daily lipid storage |
| ΔEI | | | | kJ/day | change in nominal energy intake (see main text) |

between 10 and 90% ($c = 10, 20, \dots, 90\%$). In the CIM, the energy deposit factor g_{ED} was set to 0 or 1. In the EBM-IOM control, the carbohydrate intake was set to 50% for all simulations. Overall, the virtual cohorts were simulated in 19 conditions: 18 CIM conditions and 1 EBM-IOM control. For cohort V1, time ranged between 0 and 15 years, with data collection at baseline, 0, 3 and 15 years. The nominal energy intake EI_{50} was varied according to a Gaussian distribution around the baseline energy intake (Table S2). For cohort V2, time ranged between 0 and 5 years, with data collection at baseline, 0, 2, and 5 years. The nominal energy intake EI_{50} was restricted to 3765.6 kJ/day (900 kcal/day, [11]) for the first 9 months, and went back up to 90% of the baseline energy intake between 9 months and 5 years. Physical activity levels were maintained constant for the duration of the simulations. For the short-term trial, a subset of cohort V1 with BMI between 30 and 50 kg/m² was simulated between time 0 and 61 days, with data collection at 0, 1, 7, 14, 31, and 61 days. The nominal energy intake was restricted by 1000kJ/day. Baseline summary statistics are reported in Table S4.

Supplementary Table S4. Statistical properties of the virtual cohorts (V1: $n = 938$; V2: $n = 687$; trial: $n = 678$).

| Quantity | V1 Mean | V1 STD | V2 Mean | V2 STD | Trial Mean | Trial STD |
|--------------|----------|---------|----------|---------|------------|-----------|
| F | 43.79 | 14.62 | 63.28 | 14.53 | 48.71 | 10.86 |
| L | 56.15 | 4.95 | 55.54 | 4.57 | 56.77 | 4.87 |
| Age | 38.44 | 7.30 | 42.62 | 9.44 | 38.66 | 7.18 |
| $Lipid\ age$ | 2.25 | 0.59 | 2.45 | 0.60 | 2.35 | 0.59 |
| BW | 100.44 | 17.06 | 119.32 | 15.00 | 105.98 | 13.58 |
| BMI | 34.91 | 6.80 | 43.97 | 6.79 | 37.26 | 4.70 |
| RMR | 7183.72 | 758.73 | 7757.00 | 682.39 | 7374.26 | 685.33 |
| EE | 11583.00 | 2471.58 | 11544.70 | 2284.94 | 11761.87 | 2508.15 |
| EI | 11585.12 | 2473.20 | 3765.60 | 0.00 | 11375.95 | 2509.48 |
| K_{in}^0 | 0.06 | 0.02 | 0.07 | 0.02 | 0.06 | 0.02 |

1.6 Statistical methods

Statistical tests are usually done to distinguish small differences between groups of limited sizes. The large size of the virtual cohorts, combined with the fact that the numerical simulations are deterministic, means that statistical power is sufficient to detect even small, non-meaningful differences. Therefore we did not apply any statistical tests for differences between groups. Instead, we used the term “significant” to denote differences that in our interpretation were large enough to have a physiological significance.

1.7 Data and code availability

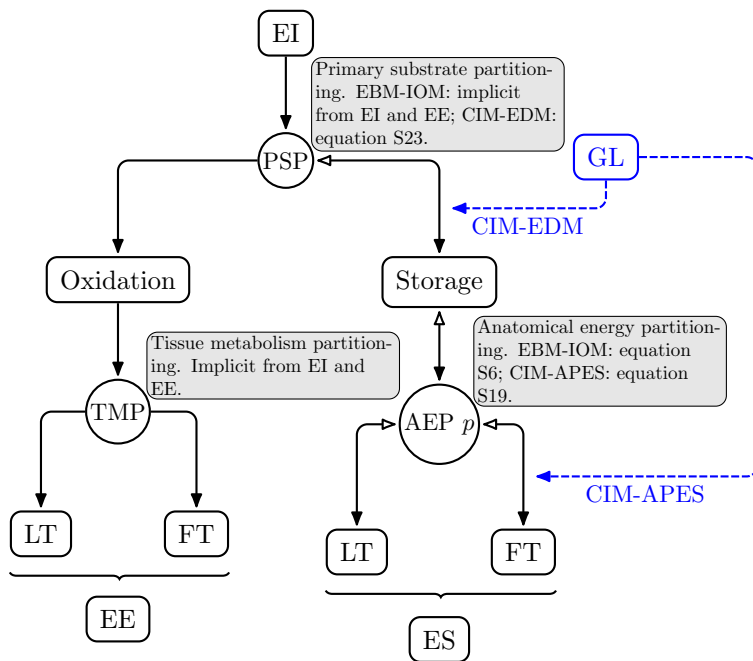
The numerical implementation of the model, the scripts to generate the datasets and the scripts to generate the tables and figures have been deposited at <https://gitlab.inria.fr/bernard1/ebm-cim-lipid>.

References

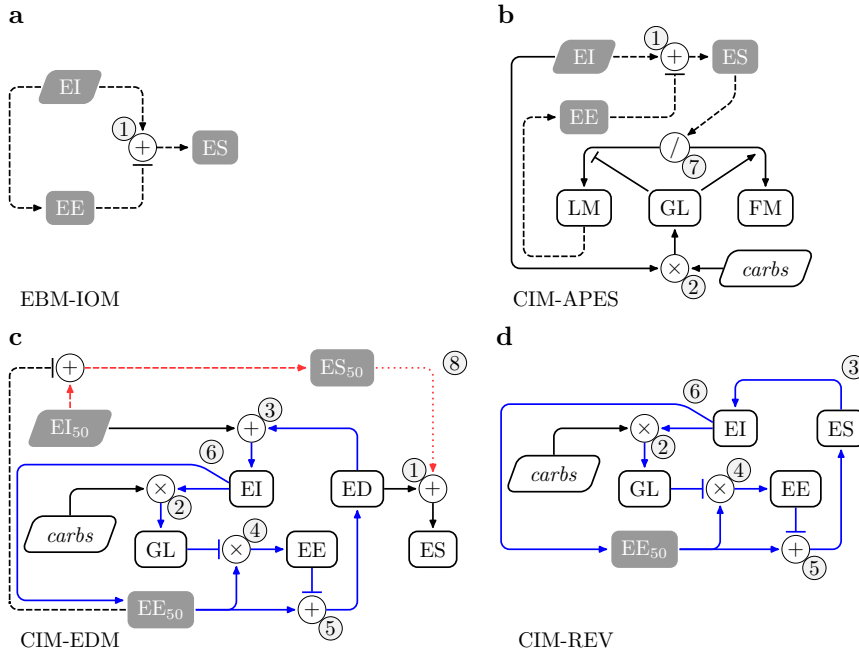
- [1] Hall KD, Sacks G, Chandramohan D, Chow CC, Wang YC, Gortmaker SL, Swinburn BA. 2011 Quantification of the effect of energy imbalance on bodyweight. *The Lancet* **378**, 826–837.
- [2] Jackson AS, Stanforth PR, Gagnon J, Rankinen T, Leon AS, Rao D, Skinner JS, Bouchard C, Wilmore JH. 2002 The effect of sex, age and race on estimating percentage body fat from body mass index: The Heritage Family Study. *International Journal of Obesity* **26**, 789–796.
- [3] Forbes G. 2003 Some adventures in body composition, with special reference to nutrition. *Acta Diabetologica* **40**, s238–s241.
- [4] Ludwig DS, Aronne LJ, Astrup A, de Cabo R, Cantley LC, Friedman MI, Heymsfield SB, Johnson JD, King JC, Krauss RM et al.. 2021 The carbohydrate-insulin model: a physiological perspective on the obesity pandemic. *The American Journal of Clinical Nutrition* **114**, 1873–1885.
- [5] Wright CN, Jaceldo-Siegl K, Mashchak A, Singh PN, Fraser GE. 2021 Validation of estimated glycaemic index and glycaemic load, stratified by race, in the Adventist Health Study-2 (AHS-2). *Public Health Nutrition* **24**, 4530–4536.
- [6] Brouwer-Brolsma EM, Berendsen AA, Sluik D, Van de Wiel AM, Raben A, De Vries JH, Brand-Miller J, Feskens EJ. 2018 The glycaemic index-food-frequency questionnaire: development and validation of a food frequency questionnaire designed to estimate the dietary intake of glycaemic index and glycaemic load: An effort by the PREVIEW Consortium. *Nutrients* **11**, 13.
- [7] Taubes G. 2007 *Good calories, bad calories*. Anchor.
- [8] Ludwig DS, Friedman MI. 2014 Increasing adiposity: consequence or cause of overeating?. *Jama* **311**, 2167–2168.
- [9] Yang Y, Atasoy D, Su HH, Sternson SM. 2011 Hunger states switch a flip-flop memory circuit via a synaptic AMPK-dependent positive feedback loop. *Cell* **146**, 992–1003.
- [10] Arner P, Bernard S, Salehpour M, Possnert G, Liebl J, Steier P, Buchholz BA, Eriksson M, Arner E, Hauner H, Skurk T, Rydén M, Frayn KN, Spalding KL. 2011 Dynamics of human adipose lipid turnover in health and metabolic disease. *Nature* **478**, 110–113.

- [11] Arner P, Bernard S, Appelsved L, Fu KY, Andersson DP, Salehpour M, Thorell A, Rydén M, Spalding KL. 2019 Adipose lipid turnover and long-term changes in body weight. *Nat Med* **25**, 1385–1389.

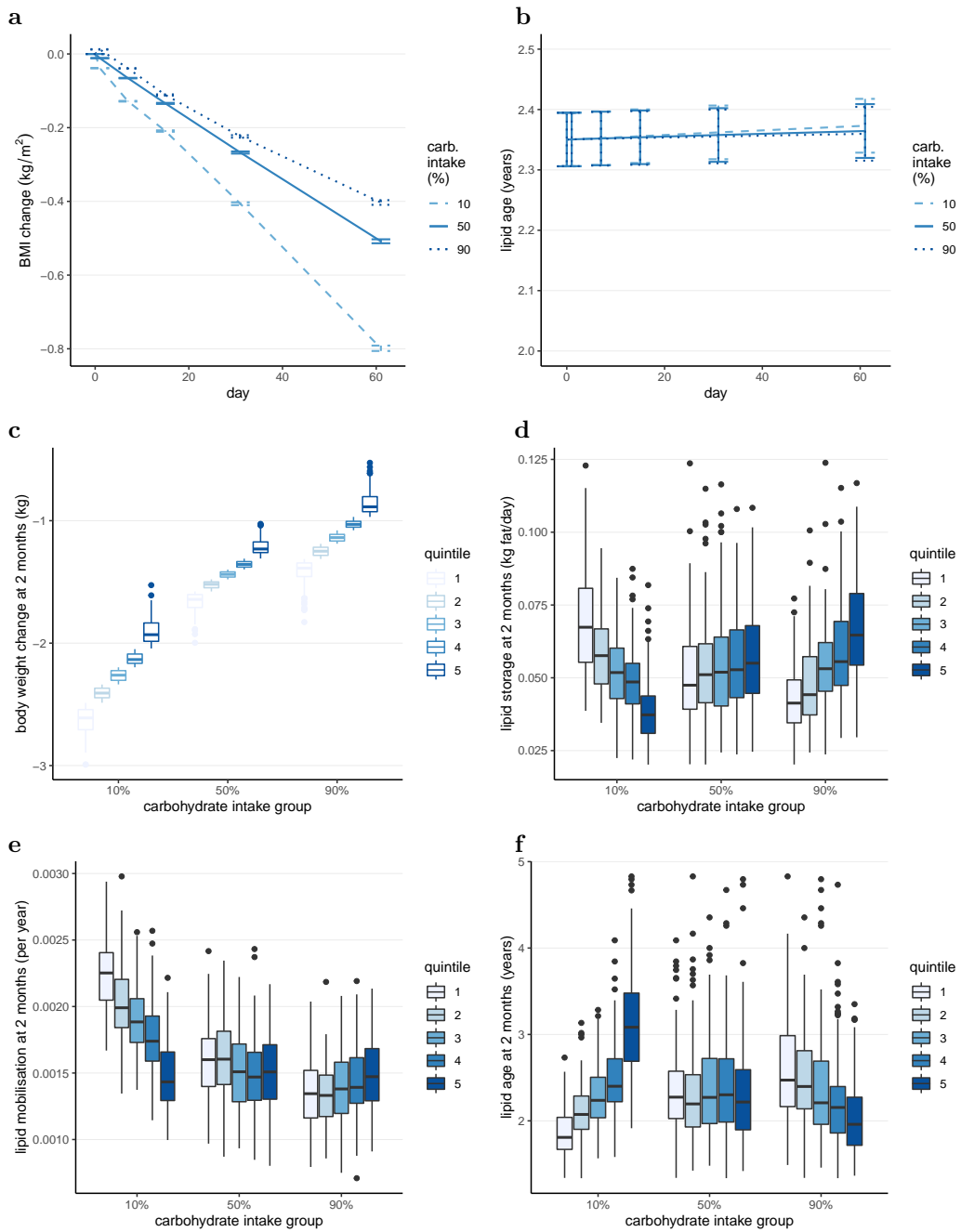
2 Supplementary figures



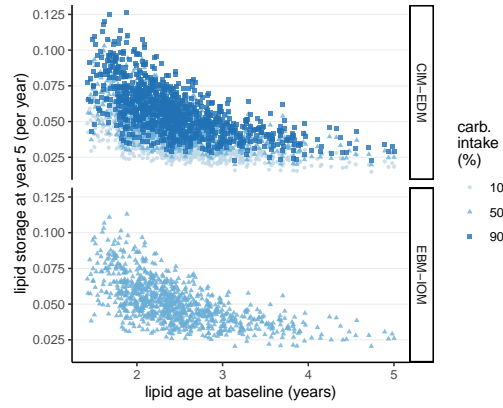
Supplementary Figure S1. Energy partition according to anatomical location and metabolic pathway. Regardless of the model and causality, total energy intake (EI) can be partitioned into energy expenditure (oxidation) and storage. Oxidation and storage can each be partitioned according to anatomical location, here lean (LT) and fat (FT) tissue. Energy conservation $ES = EI - EE$ means that ES can be positive or negative. Glycaemic load (GL) can affect primary substrate partitioning (CIM-EDM), or anatomical partitioning of energy storage (CIM-APES) or both (CIM-PDM, not shown).



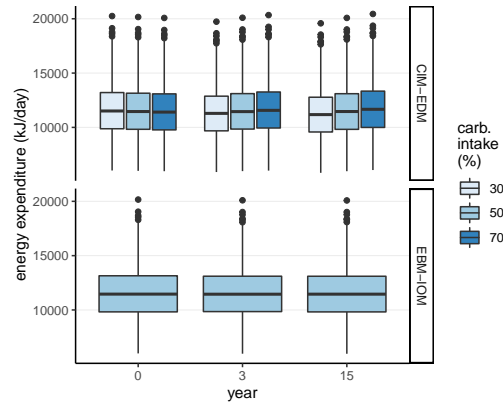
Supplementary Figure S2. Diagrams of the EBM and the CIM. The abbreviations are EI: energy intake, EE energy expenditure, ES: energy storage, carbs: percent carbohydrate intake, GL: glycaemic load, ED: energy deposit. FM: fat mass, LM: lean mass. Sharp arrow heads (\rightarrow) denote a positive action and tee arrow heads (\dashrightarrow) denote a negative action. Slanted boxes represent input model parameters. Circles represent an interaction between their incoming components: additive (+), multiplicative (\times) or divisive ($/$). Grey components are part of the EBM. Black-bordered components are specific to the CIM. **a** EBM-IOM, energy in, energy out model. **b** CIM-APES, anatomical partitioning of energy storage mechanism. **c** CIM-EDM, energy deposition mechanism. **d** CIM-REV, causation reversal mechanism. (*Point 1*, EBM-IOM, CIM-EDM, CIM-APES) The ES is determined by the difference between the EI and EE. (*Point 2*, CIM-EDM, CIM-APES, CIM-REV) The EI and carbs determine the GL. (*Point 3*, CIM-EDM, CIM-REV) The ED feeds back to EI. (*Point 4, 5*, CIM-EDM, CIM-REV) GL and EE₅₀ in determine the EE and ED. (*Point 6*, CIM-EDM, CIM-REV) The EI affects EE₅₀. (*Point 7*, CIM-APES) The GL shifts anatomical energy partitioning. (*Point 8*, CIM-EDM) Feed-forward loop.



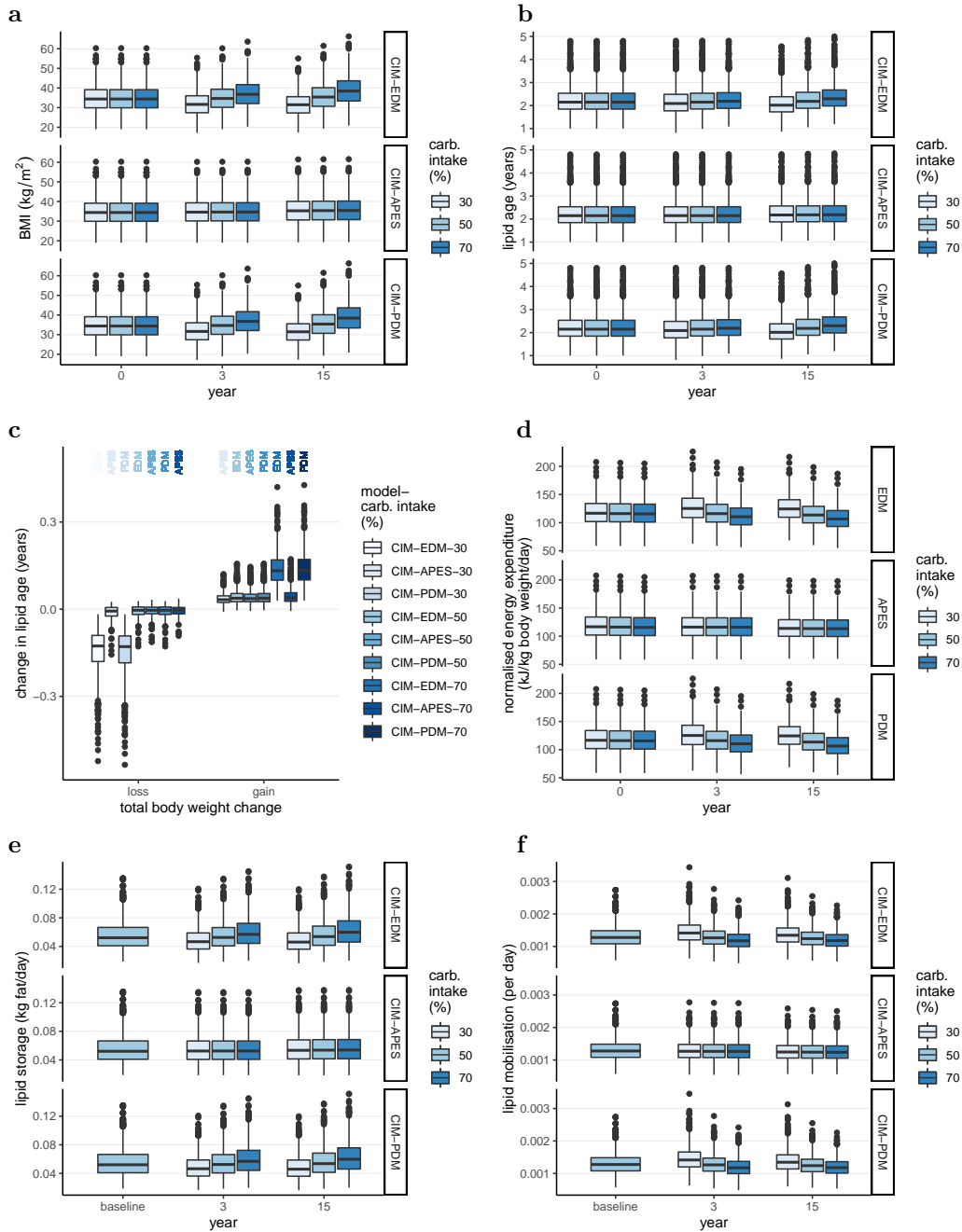
Supplementary Figure S3. Two-month virtual trial, controlled energy intake ($g_{ED} = 0$), CIM-EDM. In panels **a–d**, the grouped boxplots correspond to quintile 1 (left, most weight loss) to 5 (right, less weight loss). **a** BMI over 2 months (error bars are standard errors). **b** Lipid age over 2 months (error bars are standard errors). **c** Total body weight change at 2 months. **d** Lipid storage at 2 months. **e** Lipid mobilisation rate at 2 months. **f** Lipid age at 2 months.



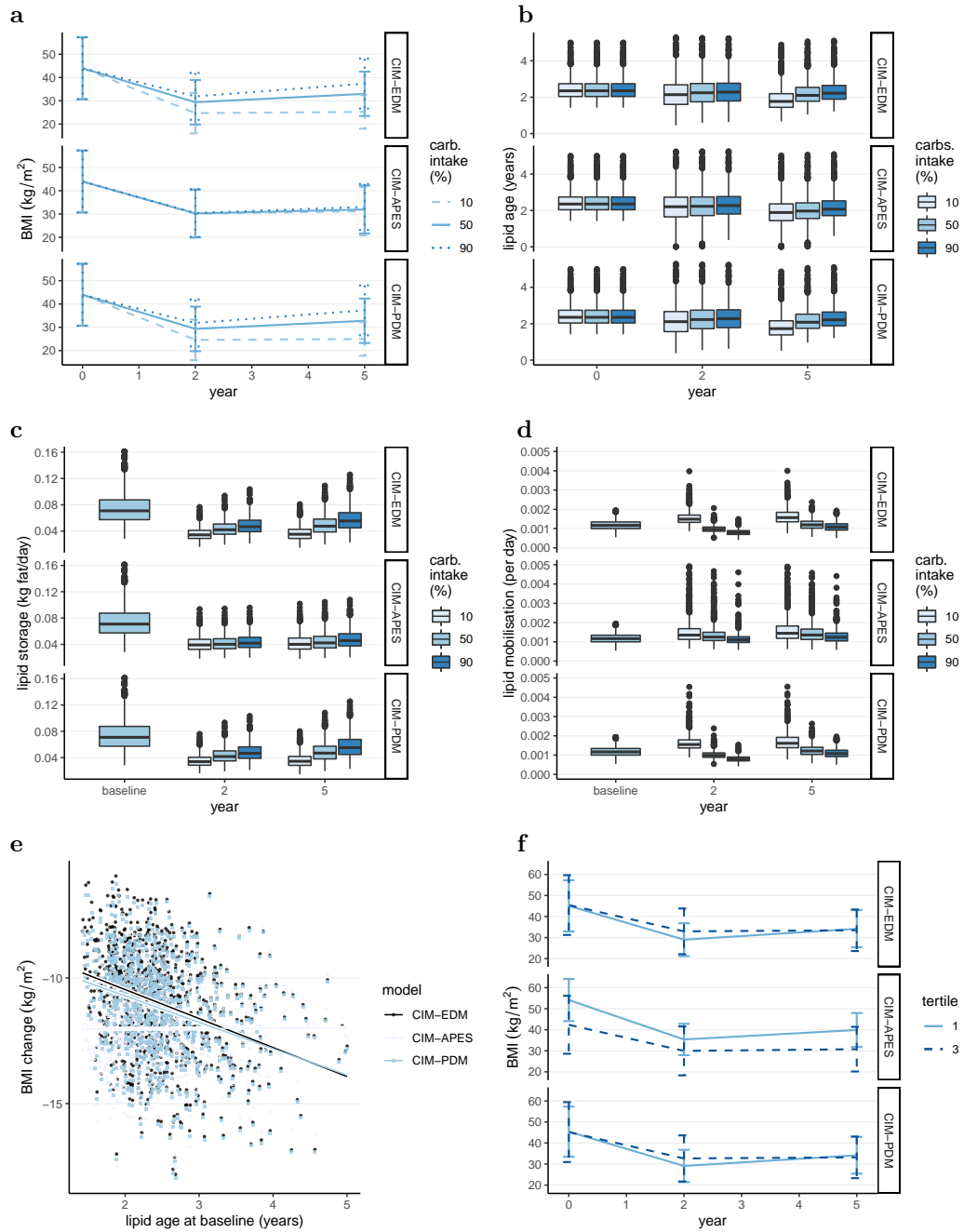
Supplementary Figure S4. Cohort V2, CIM-EDM and EBM-IOM. Inverse correlation between baseline lipid age and lipid storage rate at year 5.



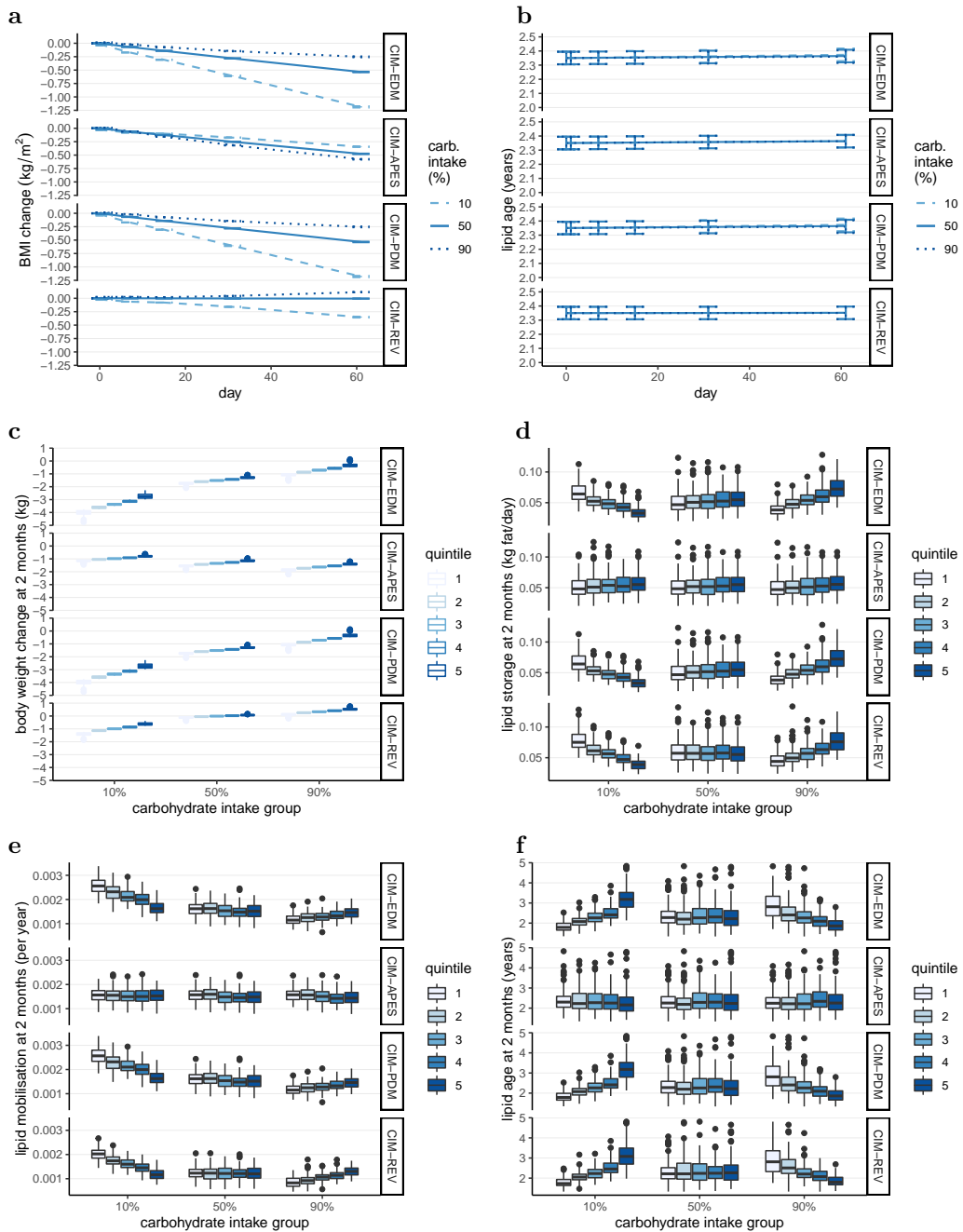
Supplementary Figure S5. Cohort V1, CIM-EDM and EBM-IOM. Energy expenditure (kJ/day).



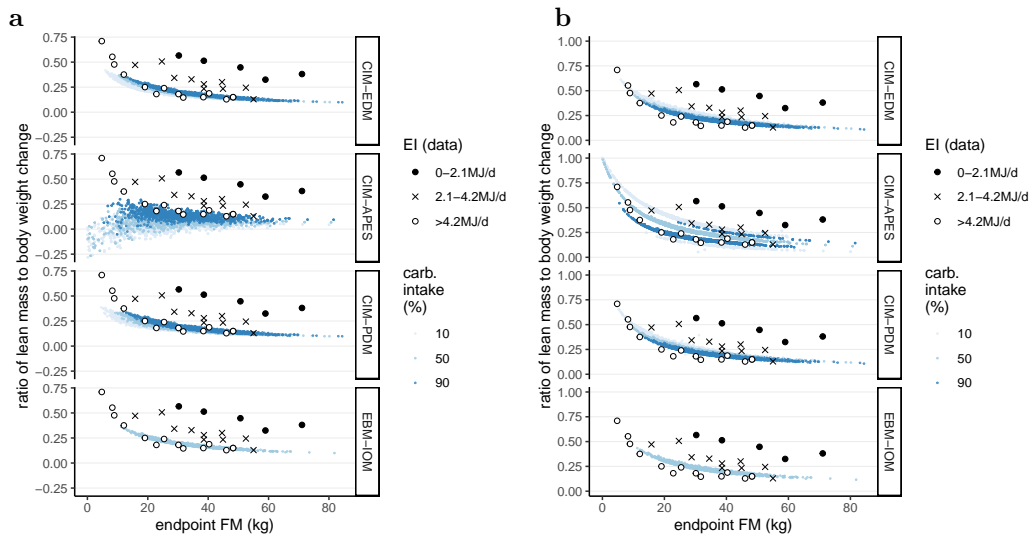
Supplementary Figure S6. Cohort V1, CIM variants. CIM-EDM: energy deposition mechanism; CIM-APES: anatomical partitioning of energy storage mechanism; CIM-PDM: combined EDM/APES. **a** BMI distribution at year 0, year 3 and year 15. **b** Lipid age at year 0, year 3 and year 15. **c** Change in lipid age in weight loss or weight gain (difference in body weight between year 15 and year 0). **d** Normalised EE (EE/BW, in kJ/kg body weight/day) with respect to carbohydrate intake at year 0, year 3 and year 15. **e** Lipid storage at baseline, year 3 and year 15. **f** Lipid mobilisation rate at baseline, year 3 and year 15.



Supplementary Figure S7. Cohort V2, CIM variants. CIM-EDM: energy deposition mechanism; CIM-APES: anatomical partitioning of energy storage mechanism; CIM-PDM: combined EDM/APES. **a** BMI at year 0, year 2, and year 5. **b** Lipid age at year 0, year 2 and year 5. **c** Lipid storage at baseline, year 2 and year 5. **d** Lipid mobilisation rate at baseline, year 2, and year 5. **e** Change in BMI between year 0 and 5, versus lipid age at baseline, with regression lines. **f** BMI at year 0, year 2, and year 5, for the first (1) and third tertile (3) of body weight change between year 2 and year 5. Tertile 1 means most weight gain. In panels e and f, carbohydrate intake is 50%.



Supplementary Figure S8. Two-month virtual trial (subset of cohort V1), controlled energy intake ($g_{ED} = 0$), CIM variants. CIM-EDM: energy deposition mechanism; CIM-APES: anatomical partitioning of energy storage mechanism; CIM-PDM: combined EDM/APES. In panels **a–d**, the grouped boxplots correspond to quintile 1 (left, most weight loss) to 5 (right, less weight loss). **a** BMI over 2 months (error bars are standard errors). **b** Lipid age over 2 months (error bars are standard errors). **c** Total body weight change at 2 months. **d** Lipid storage at 2 months. **e** Lipid mobilisation rate at 2 months. **f** Lipid age at 2 months.



Supplementary Figure S9. Cohort V2, CIM variants and EBM-IOM. The CIM variants are CIM-EDM: energy deposition mechanism; CIM-APES: anatomical partitioning of energy storage mechanism; CIM-PDM: combined EDM/APES variants. EBM-IOM: energy in, energy out model. Data on ratio of lean mass to body weight change from reference [3], Figure 2. **a** Ratio of lean mass loss to total body weight loss vs endpoint fat mass, during the weight loss period, between year 0 and year 2. **b** Ratio of lean mass loss to total body weight loss vs endpoint fat mass, during the weight gain or weight maintenance period, between year 2 and year 5. Model parameters were calibrated on daily energy intake over 4.2MJ (empty circles).